colloids and interfaces

MDPI

Article

Slow Rotation of a Soft Colloidal Sphere Normal to Two Plane Walls

Chia L. Chang and Huan J. Keh *

Department of Chemical Engineering, National Taiwan University, Taipei 10617, Taiwan
* Correspondence: huan@ntu.edu.tw; Tel.: +886-2-33663048

Abstract: The creeping flow of a viscous fluid around a soft colloidal sphere rotating about a diameter normal to two planar walls at an arbitrary position between them is theoretically investigated in the steady limit of small Reynolds numbers. The fluid velocity outside the particle consists of the general solutions of the Stokes equation in circular cylindrical and spherical coordinates, while the fluid velocity inside the porous surface layer of the particle is expressed by the general solution of the Brinkman equation in spherical coordinates. The boundary conditions are implemented first on the planar walls by means of the Hankel transforms and then at the particle and hard-core surfaces by a collocation technique. The torque exerted on the particle by the fluid is calculated as a function of the ratio of the core-to-particle radii, ratio of the particle radius to the flow penetration length of the porous layer, and relative particle-to-wall spacings over the entire range. The wall effect on the rotating soft particle can be significant. The hydrodynamic torque exerted on the confined soft sphere increases as the relative particle-to-wall spacings decrease and stays finite even when the soft sphere contacts the plane walls. It is smaller than the torque on a hard sphere (or soft one with a reduced thickness or penetration length of the porous layer), holding the other parameters constant. For a given relative wall-to-wall spacing, this torque is minimal when the particle is situated midway between the walls and rises as it locates closer to either wall.

Keywords: rotation of soft particle; boundary effect in slit; creeping flow; hydrodynamic torque

Citation: Chang, C.L.; Keh, H.J. Slow Rotation of a Soft Colloidal Sphere Normal to Two Plane Walls. *Colloids Interfaces* **2023**, *7*, 18. https://doi.org/10.3390/colloids7010018

Academic Editor: Reinhard Miller

Received: 6 February 2023
Revised: 20 February 2023
Accepted: 22 February 2023
Published: 23 February 2023

1. Introduction

The low-Reynolds-number translational and rotational motions of colloidal particles in incompressible Newtonian fluids have attracted wide attention from researchers in the fields of chemical, biomedical, mechanical, civil, and environmental engineering. These motions are practical and fundamental in numerous processes such as agglomeration, sedimentation, centrifugation, microfluidics, aerosol technology, and rheology of suspensions. The theoretical investigation of this topic began with Stokes' studies [1,2] on the creeping motions of hard spherical particles in unbounded viscous fluids. Masliyah et al. [3] and Keh and Chou [4] extended this analysis to the translation and rotation, respectively, of a soft sphere.

A soft particle of radius b has a hard core of radius a, covered by a permeable porous layer of thickness $b - a$. Polystyrene latices with surface layers [5] and biological cells with surface attachments [6] are examples of soft particles. To sterically stabilize colloidal dispersions, polymers are deliberately adsorbed by particles to form permeable layers [7]. When the porous layers of soft spheres disappear, the particles revert to hard spheres. When the hard cores of soft spheres vanish, they become fully porous spheres (like permeable colloid flocs and polymer coils) [8].

The hydrodynamic torque on a soft sphere of radius b (a hard core of radius a covered by a porous layer of thickness $b - a$) rotating with an angular velocity of Ω about a diameter in an unbounded fluid of viscosity η at low Reynolds numbers is [4]

$$T_0 = \frac{8\pi\eta\lambda^{-2}b\Omega R}{\lambda a\cosh(\lambda b - \lambda a) + \sinh(\lambda b - \lambda a)}, \tag{1}$$

where,

$$R = (\lambda^3 ab^2 - 3\lambda b + 3\lambda a)\cosh(\lambda b - \lambda a) + (\lambda^2 b^2 - 3\lambda^2 ab + 3)\sinh(\lambda b - \lambda a), \tag{2}$$

and $1/\lambda$ is the penetration length (square root of permeability) of fluid flow within the surface layer of the soft particle (T_0 and Ω are in opposite directions). In the limiting case $\lambda b \to \infty$, Equation (1) degenerates to the Stokes result for a hard sphere of radius b.

In real situations of the rotation of particles, the surrounding fluid is bounded by solid walls [9–12]. Thus, it is necessary to know whether the proximity of boundary walls meaningfully affects particle rotation. The slow rotations of a hard sphere confined by adjacent boundaries, such as in a spherical cavity [13–17], in a circular cylinder [18–20], and near one or two planar walls [13,21–23], were analyzed. Alternatively, the low-Reynolds-number rotations of a soft or porous spherical particle in a spherical cavity [4,24–27] and in a cylinder [28] were also theoretically investigated. These studies show that the effect of boundaries on the rotation of particles can be very substantial and interesting.

In the general theories of stirred vessels and rotational viscometers for highly viscous liquids, it is important to understand the variation of torque as the confinement boundary approaches. The objective of this paper is to analyze the rotation of a soft colloidal sphere (having a porous layer of arbitrary thickness and permeability) about its diameter normal to one or two plane walls at an arbitrary position between them at a low Reynolds number. The fluid velocity was found by solving the Stokes and Brinkman equations using the boundary collocation method, and semianalytical results were obtained for the hydrodynamic torque acting on the particle for various values of the relevant parameters (the core-to-particle radius ratio, shielding parameter of the porous surface layer, and relative separation distances from the walls), with excellent convergence over the entire range.

2. Analysis

As illustrated in Figure 1, we studied the creeping flow of a constant-property fluid around a soft spherical particle of radius b rotating steadily with a constant angular velocity Ω about a diameter perpendicular to two large planar walls whose distances from the particle center are c and d, respectively ($c \le d$ is taken without loss of generality), and (r, θ, φ) and (ρ, φ, z) represent the spherical and cylindrical coordinate systems, respectively, originating from the particle center. The soft sphere comprises a permeable porous surface layer of thickness $b - a$. Thus, the radius of its hard core is a. The fluid velocity inside the porous layer is finite, while the external fluid far from the particle is at rest. The objective is to find the correction to Equation (1) for the particle rotation caused by the confining plane walls.

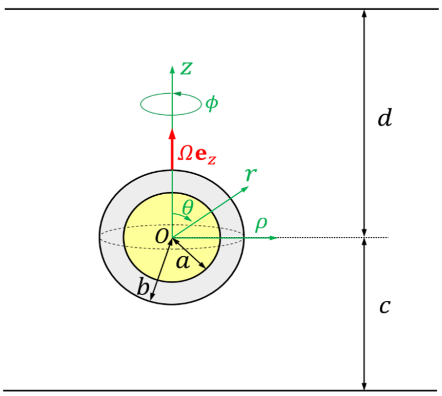

Figure 1. Geometrical sketch of a soft spherical particle rotating about a diameter normal to two planar walls.

The creeping flow is governed by the Stokes and Brinkman equations, yielding

$$[\nabla^2 - \rho^{-2} - h(r)\lambda^2]v_\phi = \frac{1}{r^2}\frac{\partial}{\partial r}(r^2\frac{\partial v_\phi}{\partial r}) + \frac{1}{r^2}\frac{\partial}{\partial \theta}[\frac{1}{\sin\theta}\frac{\partial}{\partial \theta}(v_\phi \sin\theta)] - h(r)\lambda^2 v_\phi = 0, \quad (3)$$

where $v_\phi(\rho, z)$ in cylindrical coordinates or $v_\phi(r, \theta)$ in spherical coordinates is the ϕ (only nontrivial) component of the fluid velocity distribution, the continuity equation is satisfied, the dynamic pressure is constant everywhere, λ^{-1} is the penetration length (square root of permeability) of fluid flow within the surface layer, and $h(r)$ equals unity as $a < r < b$ and zero otherwise. The boundary conditions require that the fluid is no slip at the hard-core surface and plane walls, and that both velocity and stress are continuous at the particle surface. Thus,

$$r = a\colon\ v_\phi = 0, \quad (4)$$

$$r = b\colon\ v_\phi \text{ and } \tau_{r\phi} \text{ are continuous}, \quad (5)$$

$$z = -c,\ d\colon\ v_\phi = -\Omega\rho, \quad (6)$$

$$\rho \to \infty \text{ and } -c < z < d\colon\ v_\phi = -\Omega\rho, \quad (7)$$

where $\tau_{r\phi}$ is the nontrivial shear stress at the particle surface. Equations (3)–(7) take the reference frame rotating with the particle.

The fluid velocity can be expressed in the form [23,27]

$$v_\phi = \sum_{n=1}^{\infty} (\lambda r)^{-1/2}[C_n I_{n+1/2}(\lambda r) + D_n K_{n+1/2}(\lambda r)]P_n^1(\cos\theta) \quad \text{if } a \le r \le b, \quad (8)$$

$$v_\phi = -\Omega\rho + \lambda^{-2}\int_0^\infty [X(\omega)e^{\omega z} + Y(\omega)e^{-\omega z}]\omega J_1(\omega\rho)d\omega + \sum_{n=1}^{\infty} A_n(\lambda r)^{-n-1}P_n^1(\cos\theta)$$
$$\text{if } r \ge b \text{ and } -c \le z \le d, \quad (9)$$

where P_n^1 is the associated Legendre function of the first kind of order n and degree 1, J_n is the Bessel function of the first kind of order n, I_n and K_n are the modified Bessel functions of the first and second kinds, respectively, of order n, $X(\omega)$, $Y(\omega)$, A_n, C_n, and D_n (all having the dimension of velocity) are the unknown functions and constants, respectively, to be determined. The parts of v_ϕ involving P_n^1 in the previous equations are separable solutions to Equation (3) in spherical coordinates that represent the disturbance generated by the particle and the part of v_ϕ involving J_n in Equation (9) is a Fourier-Bessel integral solution to Equation (3) in cylindrical coordinates representing the disturbance produced by the planar walls. Note that Equation (9), which is a superposition of the general solutions in cylindrical and spherical coordinates due to the linearity of Equation (3), satisfies Equation (7) immediately.

Substitution of boundary condition (6) into Equation (9) leads to

$$\int_0^\infty [X(\omega)e^{-\omega c} + Y(\omega)e^{\omega c}]\omega J_1(\omega\rho)d\omega = -\lambda^2\sum_{n=1}^{\infty} A_n\alpha_n(\rho, -c), \quad (10)$$

$$\int_0^\infty [X(\omega)e^{\omega d} + Y(\omega)e^{-\omega d}]\omega J_1(\omega\rho)d\omega = -\lambda^2\sum_{n=1}^{\infty} A_n\alpha_n(\rho, d), \quad (11)$$

where

$$\alpha_n(\rho, z) = [\lambda^2(\rho^2 + z^2)]^{-(n+1)/2}P_n^1[\frac{z}{(\rho^2 + z^2)^{1/2}}]. \quad (12)$$

The application of the Hankel transform on the variable ρ to Equations (10) and (11) yields

$$X(\omega)e^{-\omega c} + Y(\omega)e^{\omega c} = -\lambda^2\sum_{n=1}^{\infty} A_n\int_0^\infty \alpha_n(\rho, -c)\rho J_1(\omega\rho)d\rho, \quad (13)$$

$$X(\omega)\mathrm{e}^{\omega d} + Y(\omega)\mathrm{e}^{-\omega d} = -\lambda^2 \sum_{n=1}^{\infty} A_n \int_0^{\infty} \alpha_n(\rho, d)\rho J_1(\omega\rho)\mathrm{d}\rho. \tag{14}$$

The solution of Equations (13) and (14) leads to

$$X(\omega) = \sum_{n=1}^{\infty} A_n X_n(\omega), \tag{15}$$

$$Y(\omega) = \sum_{n=1}^{\infty} A_n Y_n(\omega), \tag{16}$$

where

$$X_n(\omega) = \frac{\mathrm{e}^{\omega c}[-B_n(\omega, -c) + \mathrm{e}^{\omega(c+d)} B_n(\omega, d)]}{-1 + \mathrm{e}^{2\omega(c+d)}}, \tag{17}$$

$$Y_n(\omega) = \frac{\mathrm{e}^{\omega d}[\mathrm{e}^{\omega(c+d)} B_n(\omega, -c) - B_n(\omega, d)]}{-1 + \mathrm{e}^{2\omega(c+d)}}, \tag{18}$$

and

$$B_n(\omega, z) = \frac{\mathrm{e}^{-\omega|z|}}{(n-1)!} \left(\frac{\omega|z|}{\lambda z}\right)^{n-1}. \tag{19}$$

Substitution of Equations (15) and (16) back into Equation (9) results in

$$v_\phi = -\Omega\rho + \sum_{n=1}^{\infty} A_n \gamma_n(r, \theta) \text{ if } r \geq b \text{ and } -c \leq z \leq d, \tag{20}$$

where

$$\gamma_n(r, \theta) = \lambda^{-2} \int_0^{\infty} [X_n(\omega)\mathrm{e}^{\omega r \cos\theta} + Y_n(\omega)\mathrm{e}^{-\omega r \cos\theta}]\omega J_1(\omega r \sin\theta)\mathrm{d}\omega + (\lambda r)^{-n-1} P_n^1(\cos\theta), \tag{21}$$

in which the integral can be calculated numerically.

The remaining boundary conditions to be fulfilled are those at the particle and hard core surfaces. Substituting Equations (8) and (20) into Equations (4) and (5) yields

$$\sum_{n=1}^{\infty} [C_n I_{n+1/2}(\lambda a) + D_n K_{n+1/2}(\lambda a)]\ (\lambda a)^{-1/2} P_n^1(\cos\theta) = 0, \tag{22}$$

$$\sum_{n=1}^{\infty} \{[C_n I_{n+1/2}(\lambda b) + D_n K_{n+1/2}(\lambda b)](\lambda b)^{-1/2} P_n^1(\cos\theta) - A_n \gamma_n(b, \theta)\} = -\Omega b \sin\theta, \tag{23}$$

$$\begin{aligned} \sum_{n=1}^{\infty} \{[C_n\{\lambda b I_{n-1/2}(\lambda b) + \lambda b I_{n+3/2}(\lambda b) - 3I_{n+1/2}(\lambda b)\} - D_n\{\lambda b K_{n-1/2}(\lambda b) \\ +\lambda b K_{n+3/2}(\lambda b) + 3K_{n+1/2}(\lambda b)\}](\lambda b)^{-1/2} P_n^1(\cos\theta) - 2A_n \gamma_n^*(b, \theta)\Big\} = 0, \end{aligned} \tag{24}$$

where

$$\begin{aligned} \gamma_n^*(r, \theta) = r^2 \frac{\partial}{\partial r}\left[\frac{\gamma_n(r, \theta)}{r}\right] = \lambda^{-2} r \int_0^{\infty} \Big\{[X_n(\omega)\mathrm{e}^{\omega r \cos\theta} - Y_n(\omega)\mathrm{e}^{-\omega r \cos\theta}] J_1(\omega r \sin\theta) \cos\theta \\ -[X_n(\omega)\mathrm{e}^{\omega r \cos\theta} + Y_n(\omega)\mathrm{e}^{-\omega r \cos\theta}] J_2(\omega r \sin\theta) \sin\theta\Big\}\omega^2 \mathrm{d}\omega - (\mathrm{n}+2)(\lambda r)^{-n-1} P_n^1(\cos\theta) \end{aligned} \tag{25}$$

The satisfaction of boundary conditions (22)–(24) at the inner and outer surfaces of the porous layer of the soft sphere requires solutions of the constants A_n, C_n, and D_n. The collocation technique [29] permits these boundary conditions to be imposed at N points on the meridian semicircle of each surface and the infinite series in Equations (8) and (20) to be truncated after N terms, leading to $3N$ simultaneous linear algebraic equations. These algebraic equations can be numerically solved for sufficiently large N to result in the $3N$

constants A_n, C_n, and D_n. The details of the boundary collocation scheme were given in an early paper [30] for a hard sphere translating perpendicular to two parallel plane walls.

The hydrodynamic torque acting on the soft sphere is [27]

$$T = 8\pi\eta\lambda^{-2}A_1, \tag{26}$$

where η is the viscosity of the fluid and only the lowest-order constant A_1 makes a contribution.

When the surface layer of the soft sphere vanishes, it degenerates to a hard sphere of radius $b = a$, the constants $C_n = D_n = 0$, Equations (5), (8), (22), (24), and (25) are trivial, and just Equation (23) is required to be solved for the N constants A_n. When the hard core vanishes, the soft sphere reduces to an entirely porous sphere of radius b, the constants $D_n = 0$, Equations (4) and (22) become trivial, and only Equations (23) and (24) need to be solved for the $2N$ constants A_n and C_n.

3. Results and Discussion

The numerical solutions for the hydrodynamic torque T acting on a soft spherical particle rotating about its diameter perpendicular to two plane walls as a function of the ratio of the particle radius to the porous layer penetration length λb, ratio of the core-to-particle radii a/b, particle-wall spacing parameter b/c, and relative position parameter $c/(c+d)$ obtained from the boundary collocation method, are provided in Tables A1 and A2 in Appendix A for the distinct case of $a = 0$ (a fully porous sphere) and the general case, respectively. The torque T_0, given by Equation (1) for the soft sphere in the unbounded fluid is used to normalize T. The accuracy and convergence behavior of the collocation technique depends upon the relevant parameters. All the results obtained converge to at least six significant figures. For the most difficult case, the number of collocation points, $N = 46$, is sufficiently large to achieve this convergence. These results are the same as those obtained for a hard sphere [23] in the limiting case of $\lambda b \to \infty$ or $a = b$. Obviously, $T/T_0 = 1$ is the limit $b/c = 0$, regardless of other parameters. The wall effects on the rotational motion of the soft sphere can be significant.

The normalized torque T/T_0 for a fully porous sphere rotating about its diameter perpendicular to two planar walls is plotted against the parameters λb, b/c, $c/(c+d)$ in Figures 2–4, respectively, over the entire range. For fixed values of b/c and $c/(c+d)$, as expected and shown in Table A1 and Figures 2a,b, 3a and 4b, T/T_0 is a monotonically increasing function of the shielding parameter λb (decreasing function of the permeability) for the fluid in the porous particle from unity (with $T = T_0 = 0$) at $\lambda b = 0$ to a larger finite value as $\lambda b \to \infty$. When λb is smaller than unity, the variation of T/T_0 with b/c and $c/(c+d)$ is weak (<1.4%). T/T_0 of a porous sphere with low permeability (say, $\lambda b > 100$) in general is close to that of a hard one (with $\lambda b \to \infty$), though their difference can be noticeable when the particle is very close to a wall ($b/c \to 1$).

For the given values of λb and $c/(c+d)$, as indicated in Table A1 and Figures 2b, 3a,b and 4a, the normalized torque T/T_0, acting on the confined porous sphere, is an increasing function of the particle-to-wall spacing parameter b/c from unity at $b/c = 0$ to a greater finite value at $b/c = 1$ (note that T/T_0 is still finite even for the limit that the particle touches the plane walls), since the hydrodynamic hindrance caused by the plane walls is stronger when they locate closer to the particle. The dependence of T/T_0 on b/c is robust when λb is large but vanishes in the limit $\lambda b = 0$. The supposition that the two-wall effect on the rotation of a particle can be viewed as a sum of single-wall effects will overestimate the hydrodynamic torque exerted on the particle. That is, the increase in T/T_0 from unity for the two-equidistant-wall case $c/(c+d) = 1/2$ is less than twice that for the corresponding single-wall case $c/(c+d) = 0$, which can be seen in Table A1 and Figures 2a, 3b and 4a,b.

For specified values of λb and b/c, the normalized torque T/T_0 of the porous sphere increases with an increase in the parameter $c/(c+d)$ (denoting the relative position of the porous sphere between the walls) from a finite value at $c/(c+d) = 0$ (the case of a single wall) to a greater one at $c/(c+d) = 1/2$ (the case of two equally distant walls). Namely, the nearness of a second wall will enhance the torque acting on the particle close to the first wall. The variation of T/T_0 with $c/(c+d)$ can be significant when the value of λb is large, though it disappears in the limits $\lambda b = 0$ and $b/c = 0$. For a given value of $2b/(c+d)$ (the ratio of the particle diameter to the wall-to-wall distance), as revealed by the dashed curves in Figure 4a, the torque is minimum when the particle locates in the middle between the two walls [$c/(c+d) = 1/2$] and increases monotonically as the particle approaches either wall.

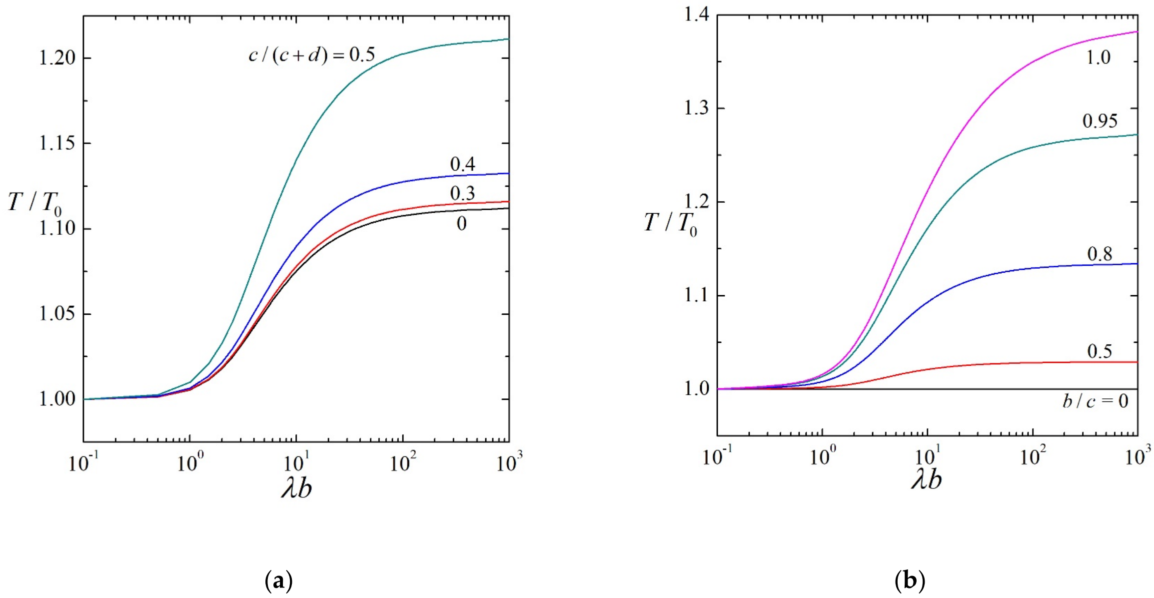

Figure 2. Normalized torque T/T_0 for a porous sphere ($a = 0$) rotating about a diameter perpendicular to two planar walls vs. the shielding parameter λb: (**a**) $b/c = 9/10$; (**b**) $c/(c+d) = 1/2$.

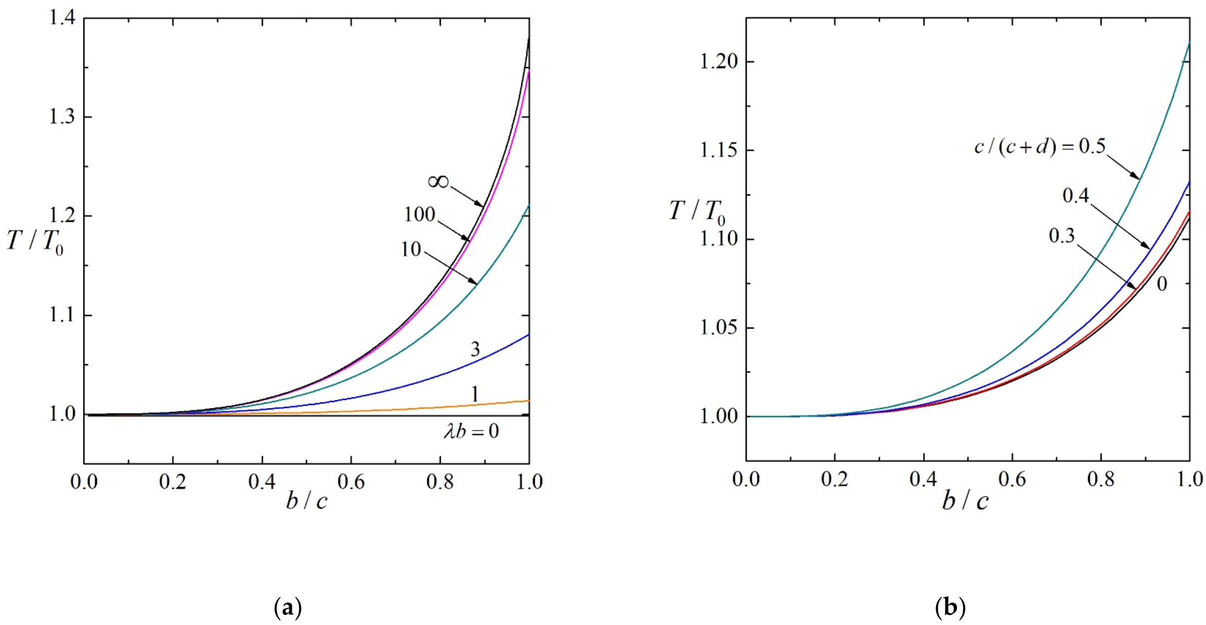

Figure 3. Normalized torque T/T_0 for a porous sphere ($a = 0$) rotating about a diameter perpendicular to two planar walls vs. the spacing parameter b/c: (**a**) $c/(c+d) = 1/2$; (**b**) $\lambda b = 10$.

After understanding the hydrodynamic effect of two parallel plane walls on the axially symmetric rotation of a porous particle, we study the general case of that on a rotating soft particle. The results of the normalized torque T/T_0 on a soft sphere rotating about its diameter perpendicular to two planar walls for different values of the core-to-particle radius ratio a/b, shielding parameter in the porous layer λb, dimensionless spacing parameter

b/c, and relative position parameter $c/(c+d)$ are presented in Figures 5–8 (together with Table A2), respectively, over the entire ranges. Again, T/T_0 increases as b/c increases from unity at $b/c = 0$ to a finite value at $b/c = 1$ and increases as $c/(c+d)$ increases from a finite value at $c/(c+d) = 0$ to another at $c/(c+d) = 1/2$, keeping the other parameters unchanged. Also, T/T_0 is a monotonic increasing function of λb from a constant (equal to zero for the entirely porous limit $a/b = 0$) at $\lambda b = 0$ (the porous surface layer is completely permeable) to a great one as $\lambda b \to \infty$ (the surface layer is impermeable).

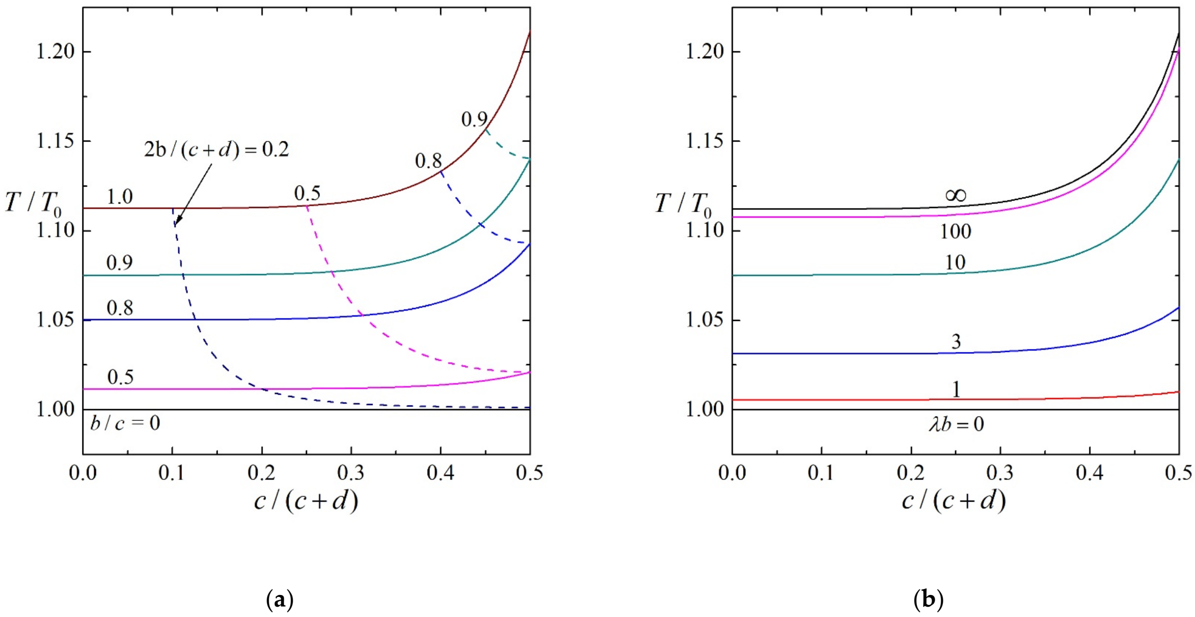

Figure 4. Normalized torque T/T_0 for a porous sphere ($a = 0$) rotating about a diameter perpendicular to two planar walls vs. the relative position parameter $c/(c+d)$: (**a**) $\lambda b = 10$, where the dashed curves show given values of $2b/(c+d)$ (the ratio of the particle diameter to the wall-to-wall distance); (**b**) $b/c = 9/10$.

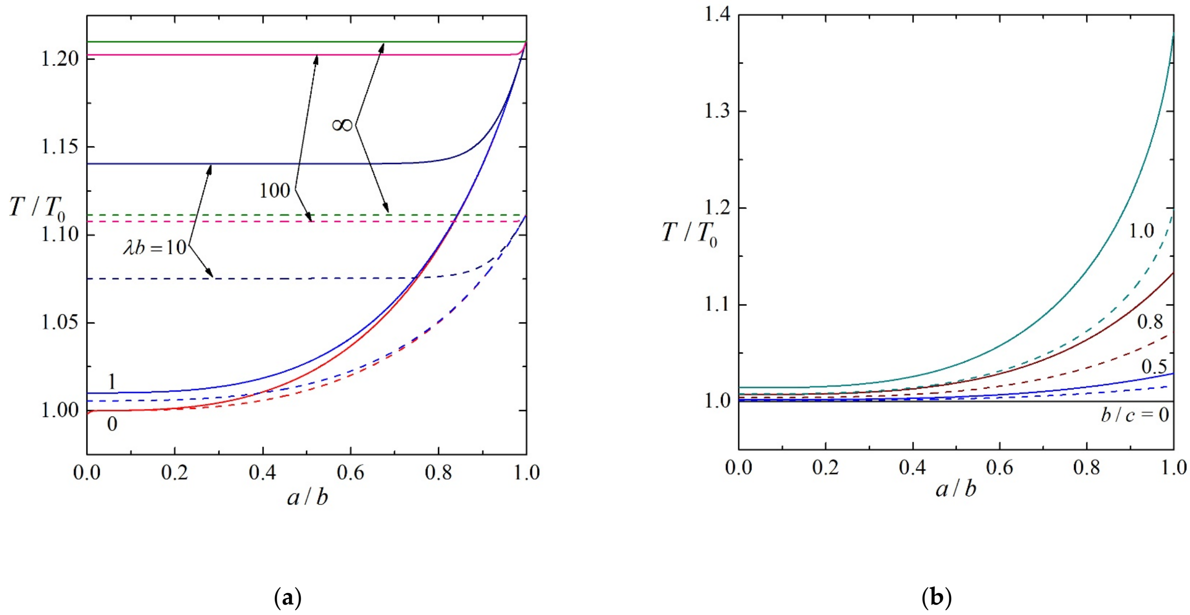

Figure 5. Normalized torque T/T_0 for a soft sphere rotating about a diameter perpendicular to two planar walls vs. the ratio of the core-to-particle radii a/b: (**a**) $b/c = 9/10$; (**b**) $\lambda b = 1$. The solid and dashed curves denote cases $c/(c+d) = 1/2$ and $c/(c+d) = 0$, respectively.

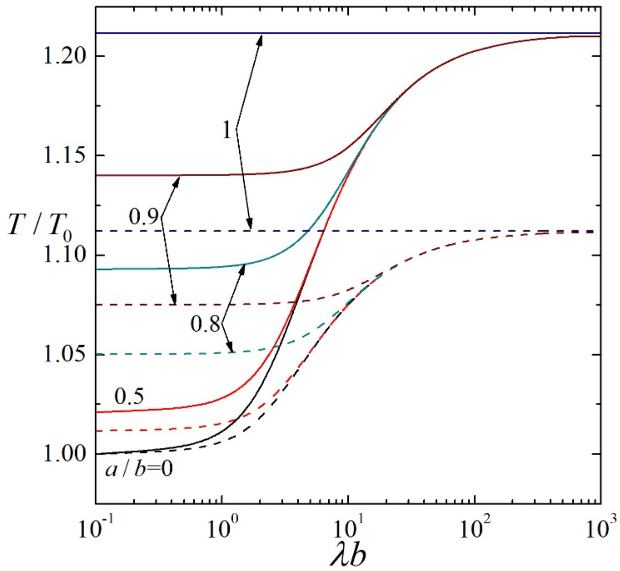

Figure 6. Normalized torque T/T_0 for a soft sphere rotating about a diameter perpendicular to two planar walls vs. the shielding parameter λb with $b/c = 9/10$. The solid and dashed curves denote cases of $c/(c+d) = 1/2$ and $c/(c+d) = 0$, respectively.

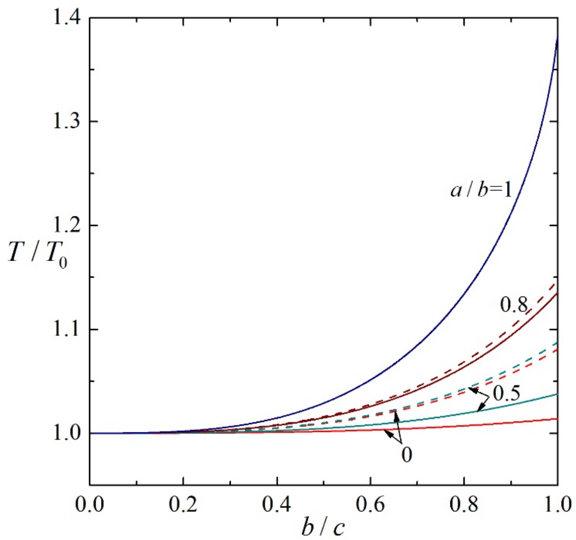

Figure 7. Normalized torque T/T_0 for a soft sphere rotating about a diameter perpendicular to two planar walls vs. the spacing parameter b/c with $c/(c+d) = 1/2$. The solid and dashed curves denote cases of $\lambda b = 1$ and $\lambda b = 3$, respectively.

For fixed values of λb, b/c, and $c/(c+d)$, Table A2 and Figures 5–8 show that the normalized torque T/T_0 for the confined soft spherical particle undergoing rotation increases monotonically with an increase in the ratio of the core-to-particle radii a/b, where the limits $a/b = 0$ and $a/b = 1$ denote a porous sphere and an impermeable sphere, respectively. That is, if the porous layer is thicker for specified permeability, particle size, and separation from walls, the torque exerted on the particle will be less. All results for the soft spherical particle fall between the upper and lower bounds of $a/b = 1$ and $a/b = 0$, respectively. For the circumstance where the surface layer has low to mediate permeability (e.g., $\lambda b \geq 10$), as shown in Figures 5a and 8, T/T_0 on the particle with a/b smaller than about 0.8 can be well approximated by that for a fully porous particle of the same size, permeability, and distances from walls. In this case, the relative motion of the fluid is barely felt by the hard core of the soft sphere, and its hindrance to the flow is negligible. However, this approximation is not valid for the porous layer with high permeability.

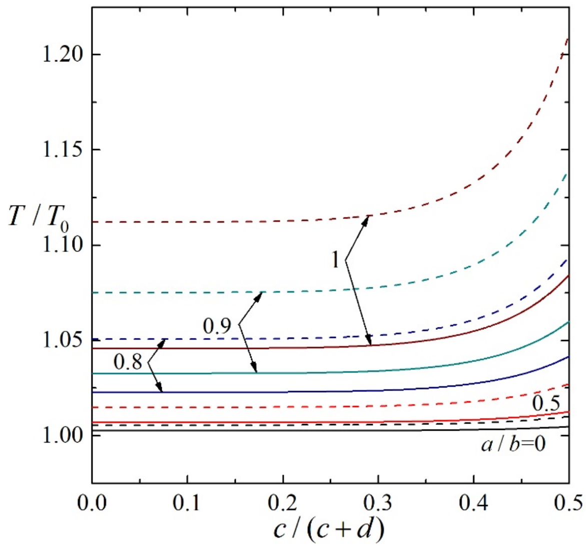

Figure 8. Normalized torque T/T_0 for a soft sphere rotating about a diameter perpendicular to two planar walls vs. the relative position parameter $c/(c+d)$ with $\lambda b = 1$. The solid and dashed curves denote cases of $b/c = 7/10$ and $b/c = 9/10$, respectively.

Recently, collocation results were obtained for the normalized hydrodynamic torque T/T_0 of a soft sphere of radius b rotating about a diameter on the axis of a circular cylinder of radius c [28]. Similar to the currently considered case of axisymmetric rotation of the particle perpendicular to two equidistant plane walls (i.e., at the center of a slit), T/T_0 is a monotonically growing function of the shielding parameter λb (from a value at $\lambda b = 0$ to a higher one at $\lambda b \to \infty$), particle-wall spacing parameter b/c (from unity at $b/c = 0$ to a greater constant at $b/c = 1$), and core-to-particle radius ratio a/b, holding other parameters constant. The particle in the circular cylinder bears much more torque than the particle in the slit does. This result manifests that the retardation to the particle rotation caused by the confinement walls is freed in both principal lateral directions of the slit, though only in an axial direction of the cylinder.

4. Concluding Remarks

The slow rotational motion of a soft spherical particle in a viscous fluid about its diameter perpendicular to one or two planar walls is semianalytically studied using the method of boundary collocation. Convergent numerical results for the torque exerted on the particle by the fluid were obtained for various values of the ratio of the particle radius to the flow penetration length of the porous layer λb, the ratio of the core-to-particle radii a/b, particle-wall spacing parameter b/c, and relative position parameter $c/(c+d)$. The wall effect on the rotating soft particle can be significant. The normalized torque, T/T_0, acting on the confined particle increases with an increase in b/c from unity as $b/c = 0$ (the particle is far from the walls) and remains finite even at the contact limit $b/c = 1$. This torque is smaller than that on a hard sphere (or soft one with larger a/b or λb), keeping the other parameters' constant. For a given ratio of the particle diameter to the wall-to-wall distance $2b/(c+d)$, T/T_0 is minimal when the particle is midway between the two walls [$c/(c+d) = 1/2$] and increases as it locates closer to either wall [the value of $c/(c+d)$ decreases]. Experimental data of the normalized torque for the slow rotation of a soft particle near one or two plane walls would be needed to confirm the validity of our semianalytical collocation results at various ranges of λb, a/b, b/c, and $c/(c+d)$.

Section three provides results for a resistance problem, where the hydrodynamic torque T on a particle rotating normal to two planar walls is considered for a given angular velocity Ω [equal to $(T_0/8\pi\eta\lambda^{-2}bR)[\lambda a\cosh(\lambda b-\lambda a)+\sinh(\lambda b-\lambda a)]$ according to Equation (1)]. In a mobility problem, the torque, T (equal to $8\pi\eta\lambda^{-2}b\Omega_0 R/[\lambda a\cosh(\lambda b-\lambda a)+\sinh(\lambda b-\lambda a)]$), imposed to the particle is assumed and the boundary-corrected angular velocity, Ω, is considered. For a soft sphere rotating normal to two plane walls dealt with here, the normalized angular velocity Ω/Ω_0 for the mobility problem is equal to $(T/T_0)^{-1}$, as given in Tables A1 and A2 and Figures 2–8 for the resistance problem.

Author Contributions: Conceptualization, H.J.K.; methodology, H.J.K. and C.L.C.; investigation, H.J.K. and C.L.C.; writing—original draft preparation, H.J.K. and C.L.C.; writing—review and editing, H.J.K.; supervision, H.J.K.; funding acquisition, H.J.K. All authors have read and agreed to the published version of the manuscript.

Funding: This research was funded by the Ministry of Science and Technology, Taiwan (Republic of China) grant number MOST 110-2221-E-002-017-MY3.

Institutional Review Board Statement: Not applicable.

Informed Consent Statement: Not applicable.

Data Availability Statement: Not applicable.

Conflicts of Interest: The authors declare no conflict of interest. The funders had no role in the design of the study; in the collection, analyses, or interpretation of data; in the writing of the manuscript; or in the decision to publish the results.

Appendix A

The collocation solutions for the normalized torque T/T_0 acting on a soft sphere rotating about its diameter perpendicular to two plane walls as a function of the ratio of the particle radius to the porous layer penetration length λb, ratio of the core-to-particle radii a/b, particle-wall spacing parameter b/c, and relative position parameter $c/(c+d)$ are presented in Tables A1 and A2 for the limiting case of $a = 0$ (a fully porous sphere) and general case, respectively.

Table A1. Normalized torque T/T_0 for a porous sphere ($a = 0$) rotating about a diameter perpendicular to two parallel planar walls.

$c/(c+d)$	b/c	T/T_0			
		λb=1	λb=10	λb=100	λb=600
0	0.1	1.00001	1.00009	1.00012	1.00012
	0.3	1.00021	1.00247	1.00329	1.00337
	0.5	1.00095	1.01156	1.01544	1.01585
	0.6	1.00165	1.02021	1.02714	1.02786
	0.7	1.00262	1.03270	1.04432	1.04554
	0.8	1.00392	1.05031	1.06937	1.07144
	0.9	1.00559	1.07526	1.10766	1.11143
	0.95	1.00659	1.09183	1.13641	1.14210
	0.99	1.00746	1.10804	1.17065	1.18075
	0.995	1.00758	1.11031	1.17647	1.18807
	0.999	1.00767	1.11218	1.18165	1.19516
1/4	0.1	1.00001	1.00009	1.00012	1.00013
	0.3	1.00021	1.00251	1.00333	1.00342
	0.5	1.00097	1.01173	1.01567	1.01607
	0.6	1.00167	1.02050	1.02753	1.02826
	0.7	1.00266	1.03317	1.04495	1.04619
	0.8	1.00397	1.05103	1.07034	1.07243
	0.9	1.00567	1.07631	1.10907	1.11289
	0.95	1.00668	1.09307	1.13811	1.14386
	0.99	1.00757	1.10946	1.17261	1.18280
	0.995	1.00769	1.11175	1.17849	1.19017
	0.999	1.00778	1.11363	1.18371	1.19734

Table A1. *Cont.*

$c/(c+d)$	b/c	T/T_0			
		λb=1	λb=10	λb=100	λb=600
1/2	0.1	1.00001	1.00016	1.00022	1.00022
	0.3	1.00037	1.00446	1.00594	1.00609
	0.5	1.00172	1.02101	1.02813	1.02886
	0.6	1.00297	1.03690	1.04972	1.05106
	0.7	1.00473	1.06007	1.08180	1.08410
	0.8	1.00708	1.09308	1.12918	1.13312
	0.9	1.01011	1.14040	1.20263	1.20992
	0.95	1.01192	1.17212	1.25847	1.26959
	0.99	1.01352	1.20337	1.32558	1.34554
	0.995	1.01373	1.20775	1.33710	1.36004
	0.999	1.01389	1.21135	1.34733	1.37420

Table A2. Normalized torque T/T_0 for a soft sphere with $\lambda b = 1$ rotating about a diameter perpendicular to two parallel planar walls.

$c/(c+d)$	b/c	T/T_0		
		a/b=0.5	a/b=0.8	a/b=0.95
0	0.1	1.00002	1.00006	1.00011
	0.3	1.00055	1.00175	1.00290
	0.5	1.00253	1.00816	1.01362
	0.6	1.00438	1.01420	1.02387
	0.7	1.00698	1.02282	1.03880
	0.8	1.01046	1.03469	1.06020
	0.9	1.01498	1.05079	1.09159
	0.95	1.01769	1.06088	1.11354
	0.99	1.02009	1.07019	1.13645
	0.995	1.02041	1.07145	1.13982
	0.999	1.02066	1.07246	1.14263
1/4	0.1	1.00002	1.00007	1.00011
	0.3	1.00055	1.00177	1.00294
	0.5	1.00256	1.00827	1.01381
	0.6	1.00444	1.01440	1.02421
	0.7	1.00708	1.02315	1.03935
	0.8	1.01061	1.03519	1.06104
	0.9	1.01520	1.05151	1.09283
	0.95	1.01794	1.06173	1.11501
	0.99	1.02038	1.07117	1.13814
	0.995	1.02070	1.07244	1.14154
	0.999	1.02096	1.07347	1.14437
1/2	0.1	1.00004	1.00012	1.00019
	0.3	1.00098	1.00316	1.00525
	0.5	1.00457	1.01479	1.02477
	0.6	1.00792	1.02584	1.04365
	0.7	1.01264	1.04172	1.07145
	0.8	1.01899	1.06378	1.11175
	0.9	1.02727	1.09397	1.17167
	0.95	1.03225	1.11304	1.21400
	0.99	1.03667	1.13074	1.25853
	0.995	1.03725	1.13313	1.26511
	0.999	1.03772	1.13507	1.27059

References

1. Stokes, G.G. On the theories of the internal friction of fluids in motion and of the equilibrium and motion of elastic solids. *Trans. Camb. Phil. Soc.* **1845**, *8*, 287–319.
2. Stokes, G.G. On the effect of the internal friction of fluids on the motion of pendulums. *Trans. Camb. Phil. Soc.* **1851**, *9*, 8–106.
3. Masliyah, J.H.; Neale, G.; Malysa, K.; van de Ven, T.G.M. Creeping flow over a composite sphere: Solid core with porous shell. *Chem. Eng. Sci.* **1987**, *42*, 245–253. [CrossRef]
4. Keh, H.J.; Chou, J. Creeping motion of a composite sphere in a concentric spherical cavity. *Chem. Eng. Sci.* **2004**, *59*, 407–415. [CrossRef]
5. Anderson, J.L.; Solomentsev, Y. Hydrodynamic effects of surface layer on colloidal particles. *Chem. Eng. Commun.* **1996**, *148–150*, 291–314. [CrossRef]
6. Wunderlich, R.W. The effects of surface structure on the electrophoretic mobilities of large particles. *J. Colloid Interface Sci.* **1982**, *88*, 385–397. [CrossRef]
7. Napper, D.H. *Polymeric Stabilization of Colloidal Dispersions*; Academic Press: London, UK, 1983.
8. Neale, G.; Epstein, N.; Nader, W. Creeping flow relative to permeable spheres. *Chem. Eng. Sci.* **1973**, *28*, 1865–1874. [CrossRef]
9. Malysa, K.; van de Ven, T.G.M. Rotational and translational motion of a sphere parallel to a wall. *Int. J. Multiph. Flow* **1986**, *12*, 459–468. [CrossRef]
10. Liu, Q.; Prosperetti, A. Wall effects on a rotating sphere. *J. Fluid Mech.* **2010**, *657*, 1–21. [CrossRef]
11. Daddi-Moussa-Ider, A.; Lisicki, M.; Gekle, S. Slow rotation of a spherical particle inside an elastic tube. *Acta Mech.* **2018**, *229*, 149–171. [CrossRef]
12. Romanò, F.; des Boscs, P.-E.; Kuhlmann, H.C. Forces and torques on a sphere moving near a dihedral corner in creeping flow. *Eur. J. Mech. B Fluids* **2020**, *84*, 110–121. [CrossRef]
13. Jeffery, G.B. On the steady rotation of a solid of revolution in a viscous fluid. *Proc. Lond. Math. Soc.* **1915**, *14*, 327–338. [CrossRef]
14. Keh, H.J.; Chang, J.H. Boundary effects on the creeping-flow and thermophoretic motions of an aerosol particle in a spherical cavity. *Chem. Eng. Sci.* **1998**, *53*, 2365–2377. [CrossRef]
15. Lee, T.C.; Keh, H.J. Slow motion of a spherical particle in a spherical cavity with slip surfaces. *Int. J. Eng. Sci.* **2013**, *69*, 1–15. [CrossRef]
16. Papavassiliou, D.; Alexander, G.P. Exact solutions for hydrodynamic interactions of two squirming spheres. *J. Fluid Mech.* **2017**, *813*, 618–646. [CrossRef]
17. Chou, C.Y.; Keh, H.J. Slow rotation of a spherical particle in an eccentric spherical cavity with slip surfaces. *Eur. J. Mech. B Fluids* **2021**, *86*, 150–156. [CrossRef]
18. Brenner, H.; Sonshine, R.M. Slow viscous rotation of a sphere in a circular cylinder. *Quart. J. Mech. Appl. Math.* **1964**, *17*, 55–63. [CrossRef]
19. Greenstein, T.; Schiavina, G.L. Torque exerted on a slowly rotating eccentrically positioned sphere within an infinitely long circular cylinder. *Int. J. Multiph. Flow* **1975**, *2*, 353–355. [CrossRef]
20. Lee, M.C.; Keh, H.J. Slow axisymmetric rotation of a sphere in a circular tube with slip surfaces. *Fluid Dyn. Res.* **2021**, *53*, 065502. [CrossRef]
21. Dean, W.R.; O'Neill, M.E. A slow motion of viscous liquid caused by the rotation of a solid sphere. *Mathematika* **1963**, *10*, 13–24. [CrossRef]
22. Chen, P.Y.; Keh, H.J. Slow motion of a slip spherical particle parallel to one or two plane walls. *J. Chin. Inst. Chem. Eng.* **2003**, *34*, 123–133.
23. Liao, J.C.; Keh, H.J. Slow rotation of a sphere about its diameter normal to two planes with slip surfaces. *Fluid Dyn. Res.* **2022**, *54*, 035502. [CrossRef]
24. Srinivasacharya, D.; Krishna Prasad, M. Steady rotation of a composite sphere in a concentric spherical cavity. *Acta Mech. Sin.* **2012**, *28*, 653–658. [CrossRef]
25. Prakash, J.; Raja Sekhar, G.P. Slow motion of a porous spherical particle with a rigid core in a spherical fluid cavity. *Meccanica* **2017**, *52*, 91–105. [CrossRef]
26. Sherief, H.H.; Faltas, M.S.; Saad, E.I. Stokes resistance of a porous spherical particle in a spherical cavity. *Acta Mech.* **2016**, *227*, 1075–1093. [CrossRef]
27. Chou, C.Y.; Keh, H.J. Low-Reynolds-number rotation of a soft particle inside an eccentric cavity. *Eur. J. Mech. B Fluids* **2022**, *91*, 194–201. [CrossRef]
28. Jhuang, L.J.; Keh, H.J. Slow axisymmetric rotation of a soft sphere in a circular cylinder. *Eur. J. Mech. B Fluids* **2022**, *95*, 205–211. [CrossRef]
29. Ganatos, P.; Weinbaum, S.; Pfeffer, R. A strong interaction theory for the creeping motion of a sphere between plane parallel boundaries Part 2 Parallel motion. *J. Fluid Mech.* **1980**, *99*, 755–783. [CrossRef]
30. Chang, Y.C.; Keh, H.J. Slow motion of a slip spherical particle perpendicular to two plane walls. *J. Fluids Struct.* **2006**, *22*, 647–661. [CrossRef]